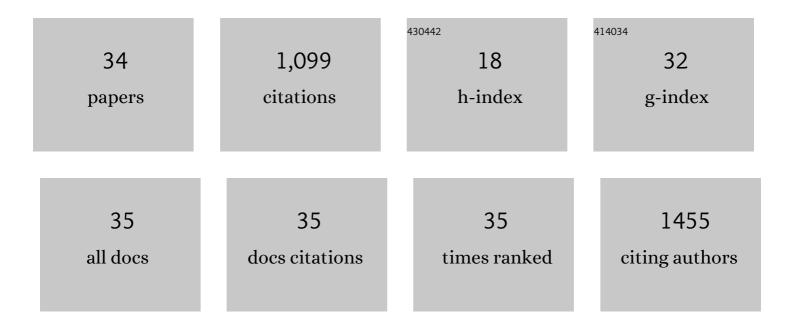
Jun Wang

List of Publications by Year in descending order

Source: https://exaly.com/author-pdf/8315808/publications.pdf Version: 2024-02-01



#	Article	IF	CITATIONS
1	Design strategies for twoâ€dimensional material photodetectors to enhance device performance. InformaÄnÃ-Materiály, 2019, 1, 33-53.	8.5	158
2	High-performance Schottky heterojunction photodetector with directly grown graphene nanowalls as electrodes. Nanoscale, 2017, 9, 6020-6025.	2.8	77
3	Visible to near-infrared photodetectors based on MoS ₂ vertical Schottky junctions. Nanotechnology, 2017, 28, 484002.	1.3	73
4	High thermochromic performance of Fe/Mg co-doped VO ₂ thin films for smart window applications. Journal of Materials Chemistry C, 2018, 6, 6502-6509.	2.7	72
5	Lightâ€Stimulated Synaptic Transistor with High PPF Feature for Artificial Visual Perception System Application. Advanced Functional Materials, 2022, 32, .	7.8	71
6	Three-Dimensional Topological Insulator Bi ₂ Te ₃ /Organic Thin Film Heterojunction Photodetector with Fast and Wideband Response from 450 to 3500 Nanometers. ACS Nano, 2019, 13, 755-763.	7.3	68
7	Enhanced Performance of Wideband Room Temperature Photodetector Based on Cd ₃ As ₂ Thin Film/Pentacene Heterojunction. ACS Photonics, 2018, 5, 3438-3445.	3.2	57
8	Ultrahigh Stability 3D TI Bi ₂ Se ₃ /MoO ₃ Thin Film Heterojunction Infrared Photodetector at Optical Communication Waveband. Advanced Functional Materials, 2020, 30, 1909659.	7.8	50
9	Highâ€Responsivity Photodetectors Based on Formamidinium Lead Halide Perovskite Quantum Dot–Graphene Hybrid. Particle and Particle Systems Characterization, 2018, 35, 1700304.	1.2	46
10	Light-modulated vertical heterojunction phototransistors with distinct logical photocurrents. Light: Science and Applications, 2020, 9, 167.	7.7	40
11	Epitaxial Topological Insulator Bi ₂ Te ₃ for Fast Visible to Mid-Infrared Heterojunction Photodetector by Graphene As Charge Collection Medium. ACS Nano, 2022, 16, 4851-4860.	7.3	35
12	Ultraviolet to Long-Wave Infrared Photodetectors Based on a Three-Dimensional Dirac Semimetal/Organic Thin Film Heterojunction. Journal of Physical Chemistry Letters, 2019, 10, 3914-3921.	2.1	29
13	Nitrogen analogues of Chichibabin's and Müller's hydrocarbons with small singlet–triplet energy gaps. Chemical Communications, 2019, 55, 7812-7815.	2.2	29
14	Spectrally and Spatially Tunable Terahertz Metasurface Lens Based on Graphene Surface Plasmons. IEEE Photonics Journal, 2018, 10, 1-8.	1.0	25
15	High responsivity and fast UV–vis–short-wavelength IR photodetector based on Cd ₃ As ₂ /MoS ₂ heterojunction. Nanotechnology, 2020, 31, 064001.	1.3	23
16	Recent Progress in 2D Inorganic/Organic Charge Transfer Heterojunction Photodetectors. Advanced Functional Materials, 2022, 32, .	7.8	23
17	Integration of green CuInS_2/ZnS quantum dots for high-efficiency light-emitting diodes and high-responsivity photodetectors. Optical Materials Express, 2018, 8, 314.	1.6	22
18	Polarimetric Three-Dimensional Topological Insulators/Organics Thin Film Heterojunction Photodetectors. ACS Nano, 2019, 13, 10810-10817.	7.3	20

Jun Wang

#	Article	IF	CITATIONS
19	Efficient Organic Upconversion Devices for Low Energy Consumption and Highâ€Quality Noninvasive Imaging. Advanced Materials, 2021, 33, e2102812.	11.1	19
20	Polarimetric Vis-NIR photodetector based on self-aligned single-walled carbon nanotubes. Carbon, 2019, 143, 844-850.	5.4	18
21	Excellent performance in vertical graphene-C60-graphene heterojunction phototransistors with a tunable bi-directionality. Carbon, 2020, 162, 375-381.	5.4	17
22	Silicon-based PbS-CQDs infrared photodetector with high sensitivity and fast response. Nanotechnology, 2020, 31, 485206.	1.3	17
23	Fabrication of hexagonal star-shaped and ring-shaped patterns arrays by Mie resonance sphere-lens-lithography. Applied Surface Science, 2018, 440, 378-385.	3.1	14
24	Optical Properties and Sensing Performance of Au/SiO2 Triangles Arrays on Reflection Au Layer. Nanoscale Research Letters, 2018, 13, 335.	3.1	12
25	Zero-Bias Visible to Near-Infrared Horizontal p-n-p TiO2 Nanotubes Doped Monolayer Graphene Photodetector. Molecules, 2019, 24, 1870.	1.7	12
26	Weyl Semiconductor Te/Sb ₂ Se ₃ Heterostructure for Broadband Photodetection and Its Binary Photoresponse by C ₆₀ as Chargeâ€Regulation Medium. Advanced Optical Materials, 2021, 9, 2101256.	3.6	12
27	A 3D topological Dirac semimetal/MoO ₃ thin film heterojunction infrared photodetector with a current reversal phenomenon. Journal of Materials Chemistry C, 2020, 8, 16024-16031.	2.7	10
28	Excellent-Performance C ₆₀ /Graphene/SWCNT Heterojunction with Light-Controlled Enhancement of Photocurrent. ACS Sustainable Chemistry and Engineering, 2020, 8, 4276-4283.	3.2	10
29	Spectral photovoltaic response of graphene-silicon heterojunction. Applied Physics Letters, 2017, 111, .	1.5	9
30	Rigorous coupled-wave analysis of absorption enhancement in vertically illuminated silicon photodiodes with photon-trapping hole arrays. Nanophotonics, 2019, 8, 1747-1756.	2.9	9
31	Highâ€Performance Photodetector based on a 3D Dirac Semimetal Cd ₃ As ₂ /Tungsten Disulfide (WS ₂) van der Waals Heterojunction. Advanced Photonics Research, 2021, 2, 2000194.	1.7	7
32	Type-III organic/two-dimensional multi-layered phototransistors with promoted operation speed at the communication band. Journal of Materials Chemistry C, 2021, 9, 13963-13971.	2.7	6
33	Deciphering the photocurrent polarity of Bi2O2Se heterojunction phototransistors to enhance detection performance. Journal of Materials Chemistry C, 0, , .	2.7	6
34	Near-infrared heterojunction field modulated phototransistors with distinct photodetection/photostorage switching features for artificial visuals. Journal of Materials Chemistry C, 2022, 10, 9198-9207.	2.7	3